Journal of Materials Chemistry A

Transparent and Flexible Organic Semiconductor Electrode with Enhanced Thermoelectric Efficiency

Journal:	*Journal of Materials Chemistry A*
Manuscript ID:	TA-ART-02-2014-000700
Article Type:	Paper
Date Submitted by the Author:	21-Feb-2014

Complete List of Authors:	Lee, Seung Hwan; Yonsei University, Department of Chemical and Biomolecular engineering Park, Hongkwan; Yonsei University, Department of Chemical and Biomolecular Engineering Kim, Soyeon; Yonsei University, Department of Chemical and Biomolecular Engineering Son, Woohyun; Yonsei University, Department of Chemical and Biomolecular Engineering Cheong, In Woo; Kyungpook National University, Kim, Jung Hyun; Yonsei University, Department of Chemical and Biomolecular Engineering

Journal of Materials Chemistry A RSCPublishing

ARTICLE

TOC

This paper describes a Sequential doping/dedoping method for the enhancement of thermoelectric properties of poly(3,4-ethylenedioxythiophene):poly(4-styrene sulfonic acid) (PEDOT:PSS) films that also permits the fabrication of transparent and flexible thermoelectric nanofilms. This method allows a precise control of both PSS concentration in the PEDOT:PSS film and its oxidation level without deterioration of the film surface defects.

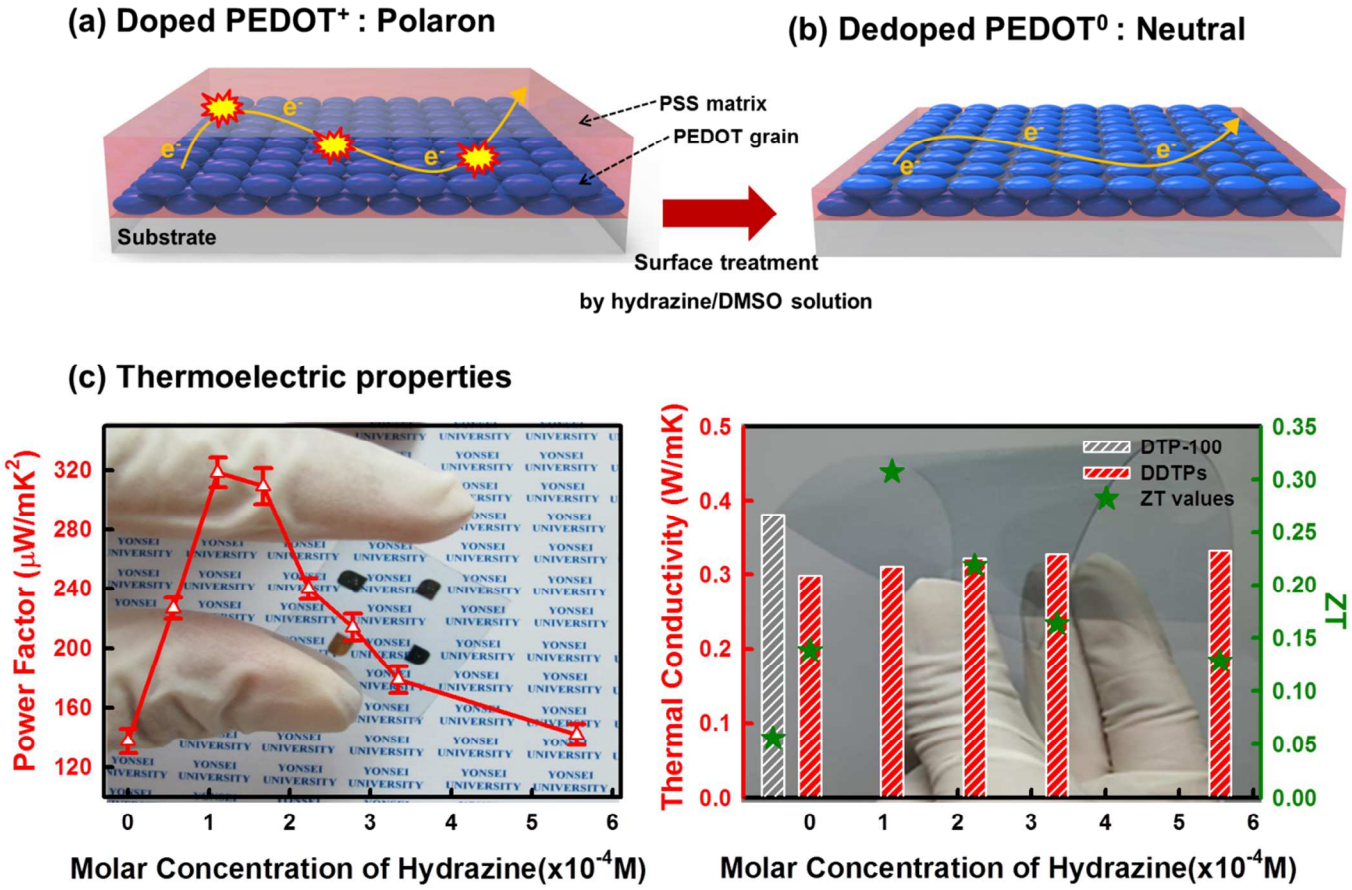

Journal of Materials Chemistry A RSCPublishing

ARTICLE

Transparent and Flexible Organic Semiconductor Nanofilms with Enhanced Thermoelectric Efficiency

Cite this: DOI: 10.1039/xoxxoooooox

Seung Hwan Lee, [a] Hongkwan Park, [a] Soyeon Kim, [a] Woohyun Son, [a] In Woo Cheong, [b,] * and Jung Hyun Kim[a,] *

Received ooth January 2012,
Accepted ooth January 2012

DOI: 10.1039/xoxxoooooox

www.rsc.org/

Sequential doping and dedoping increased the conductivity and optimized the oxidation level of transparent and flexible poly(3,4-ethylenedioxythiophene):poly(4-styrene sulfonic acid) (PEDOT:PSS) films, resulting in an improvement in the thermoelectric figure of merit ZT. The electrical conductivity (σ) increased from 970 to 1260 S/cm and the power factor from 66.5 to 70.7 $\mu W/mK^2$ at the optimum concentration of the chemical dopant *p*-toluenesulfonic acid monohydrate (TSA). Then, the doped PEDOT:PSS films were treated with hydrazine/DMSO solutions with different hydrazine concentrations to precisely control the oxidation level. During the hydrazine/DMSO treatment (dedoping), σ of the films continuously decreased from 1647 to 783 S/cm due to a decrease in the carrier concentration, whereas the Seebeck coefficient (*S*) steeply increased from 28 to 49.3 $\mu V/K$ at the optimum oxidation level. A power factor of 318.4 $\mu W/mK^2$ (σ = 1310 S/cm, *S* = 49.3 $\mu V/K$), the highest among all existing thermoelectric nanofilms, was achieved while maintaining polymer film flexibility and transparency (88.3 % of optical transmittance). In addition, the thermal conductivity (κ) of the PEDOT:PSS films decreased from 0.38 to 0.30 W/mK upon removal of the PSS. At the lowest κ value, a high ZT value of 0.31 was achieved at room temperature.

Introduction

Sustainable energy harvesting from various sources has been studied over the past several decades.[1] Recently, much attention has been devoted to harvesting technologies, which can produce electricity from various types of ambient energy that are hard to harness, such as vibration, strain, temperature gradient, and fluid flow.[2-4] Among these, thermoelectric power generation by reusing waste heat or using natural sources of heat shows considerable promise.[5-12] Improving thermoelectric conversion efficiency is crucial, hence much effort has been focused on the synthesis and characterization of thermoelectric materials with high thermoelectric figure of merit (ZT).[13]

Compared to inorganic semiconductors, conducting polymers possess several advantages as thermoelectric materials, namely low thermal conductivity, high electrical conductivity, cost-effectiveness, mass production, facile synthesis, and wide-area processing.[14-22] Among conducting polymers, for instance poly(pyrrole), poly(aniline), poly(*N*-vinylcarbazole), poly(thiophene), and poly(3,4-ethylenedioxythiophene):poly(4-styrenesulfonic acid) (PEDOT:PSS), PEDOT:PSS exhibits the highest conductivity and transparency.[23-25] The PEDOT:PSS with a higher doping level permits easy transmission of de-localized electrons through the conjugated backbone of π system.[26] It is most likely responsible for the above effect.

Doping and dedoping play an important role in the thermoelectric properties of PEDOT films, because these processes strongly affect carrier mobility and oxidation level measured by Seebeck coefficient (S) and conductivity.[27] The high values of ZT in polymers have been obtained for PEDOT:Tos reduced by chemical reduction , ZT= 0.25.[28, 29] In addition, post-treatment change of PSS concentration in case of PEDOT:PSS film is necessary because the PSS concentration required during synthesis of PEDOT is different from that for optimum thermoelectric performance of PEDOT:PSS films. Kim et al. reported a dipping method to remove PSS from the PEDOT:PSS film with ethylene glycol (EG) and dimethyl sulfoxide (DMSO), achieving a record value of ZT = 0.42.[27] Luo et al. reported a fabrication of dedoped PEDOT:PSS film via dropping method using a hydrophilic solvent/dedopant mixture.[30] To maximize the thermoelectric efficiency, oxidation level of PEDOT was also controlled electrochemically.[31] These post-treatments indeed enhanced the thermoelectric properties of PEDOT:PSS. However, they are impractical because of the inaccurate control of oxidation level, time-consuming procedure, and aggravation of the film surface defects due to swelling and detaching as a result of chemical dissolution during the dipping treatment.

This paper describes a facile chemical doping/dedoping method for the enhancement of thermoelectric properties of PEDOT:PSS coated PET thin films that also permits the fabrication of transparent and flexible thermoelectric nanofilms. This method allows a precise control of both PSS concentration in the PEDOT:PSS film and its oxidation level without deterioration of the film surface defects.

Experimental

Materials PEDOT:PSS solution (Clevios PH 1000) was purchased from Heraeus. The solid content was 1.1 wt% and the weight ratio of PEDOT to PSS was 1:2.5. *p*-Toluenesulfonic acid monohydrate (TSA, assay 98.5%), and hydrazine (35 wt% aq. solution) were purchased from Sigma-Aldrich (St Louis, MO, USA). Dimethyl sulfoxide (DMSO, 99 %) was purchased from Samchun Pure

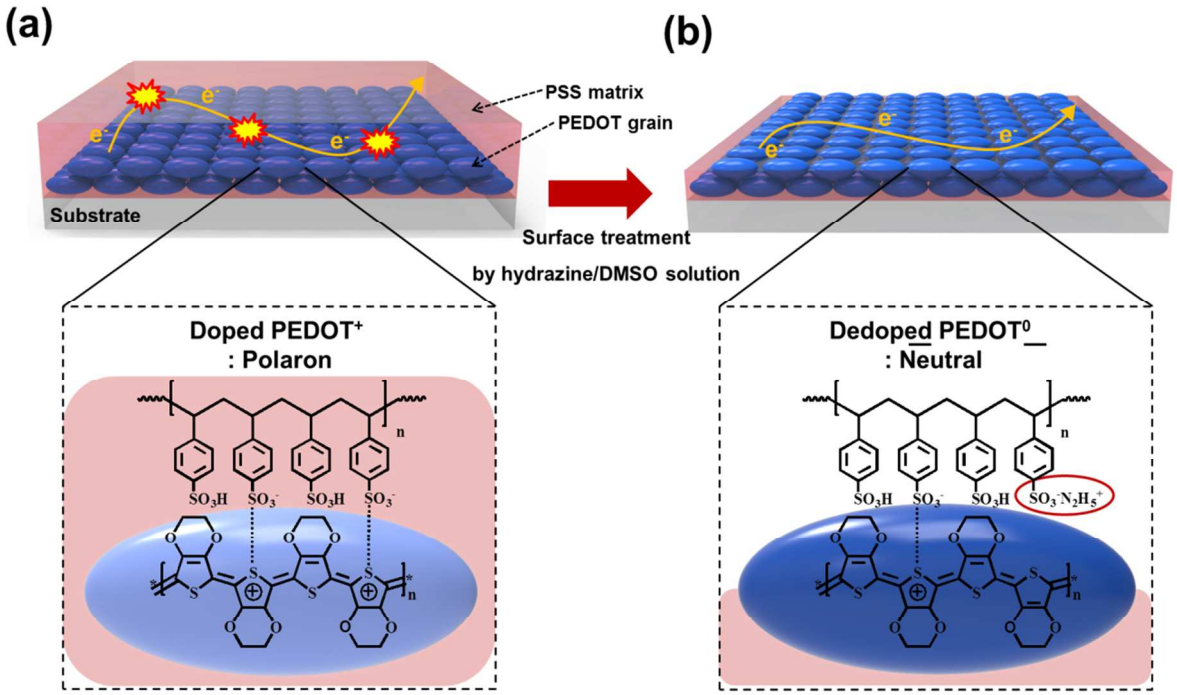

Scheme 1. An overall scheme for the spin-coated PEDOT:PSS film fabricated by the sequential treatment with TSA/DMSO doping and hydrazine/DMSO dedoping: (a) DMSO/TSA-doped PEDOT:PSS (DTP) film formation via spin coating, (b) A selective removal of PSS and dedoped PEDOT:PSS (DDTP) film treated with hydrazine/DMSO solution.

Chemicals (S. Korea). All materials were used without further purification. Double-distilled and deionized (DDI) water was used throughout the experiments.

Preparation of PEDOT:PSS Films To optimize the electrical conductivity of PEDOT:PSS in film state, a typical DMSO doping procedure with TSA concentration from 0 to 1.50 v/v% (Table 1) was followed. DMSO was added into the PEDOT:PSS aqueous solution (5.0 v/v%) and stirred gently at room temperature. The required amount of TSA (50 wt% aqueous solution) was then added drop-wise to avoid abrupt viscosity increase and subsequent poor film properties.

From the doped PEDOT:PSS solutions, PEDOT:PSS thin films were fabricated by spin coating at 1000 rpm for 30 s and the oxidation level of the film was controlled by dedoping with hydrazine/DMSO. The film thickness was ~160 nm after drying in an oven for 10 min at 150 °C. The hydrazine/DMSO solutions (0 to 5.55×10^{-4} M hydrazine concentration) were prepared by mixing. The hydrazine/DMSO solution (1000 μL) was added drop-wise onto the PEDOT:PSS film (7×7 cm^2) and the entire film surface was wetted by spin coating at 1000 rpm for 20 s. The film was then dried in an oven for 10 min at 150 °C and cooled down to room temperature. The overall procedure and effect of hydrazine/DMSO solution on PEDOT:PSS films are shown in Scheme 1.

Results and Discussion

During preparation of DMSO/TSA-doped PEDOT:PSS films, TSA/DMSO solutions (TSA concentration from 0 to 1.50 vol% at fixed DMSO concentration of 5 vol%) were mixed with a PEDOT:PSS aqueous solution. After the film preparation by spin coating, the electrical conductivity (σ), Seebeck coefficient (S) and power factor (PF) were measured (Table 1). The film thickness of the samples was ~160 nm as measured by a surface profiler.

In general, the electric conductivity (σ) of conducting polymers is proportional to carrier concentration (n) and hall mobility (μ_H): $\sigma = e\times n\times\mu_H$, where e is the electric charge.[19] TSA has been frequently used for doping of conducting polymers. TSA doping increases n by facilitating the formation of a radical cation (hole) in the PEDOT backbone thiophenes. This kind of radical cation is called polaron because the positively charged hole moves through the polymer and contributes to the conductivity. [32, 33]

DMSO-doped PEDOT:PSS film without TSA (DTP-0) exhibits σ of 970 S/cm^{-1} (Table 1), whereas DTP-100 containing 1.00 vol% TSA exhibits σ of 1218 S/cm^{-1}. A PF maximum value of 70.7 μW/mK^2 is achieved at 1.00 vol% of TSA, while S slightly decreases from 26.2 to 24.1 μV/K in comparison with DTP-0. Therefore, the DTP-100 film sample was used in the subsequent dedoping studies.

Table 1. Thermoelectric properties of PEDOT:PSS films doped with 5 vol% DMSO containing TSA at different concentrations (DTP).

Sample ID	Concentrations (vol%)		σ^b (S/cm)	S^c (μV/K)	$S^2\bullet\sigma^d$ (μW/mK^2)
	DMSO	TSA[a]			
DTP-0	5	0	970	26.2	66.5
DTP-050	5	0.50	995	25.7	65.7
DTP-075	5	0.75	1110	24.8	69.3
DTP-100	5	1.00	1218	24.1	70.7
DTP-125	5	1.25	1187	24.0	68.3
DTP-150	5	1.50	1106	23.8	62.6

[a]TSA (50 wt% aqueous solution) was used; [b]electrical conductivity; [c]Seebeck coefficient; [d]power factor (PF)

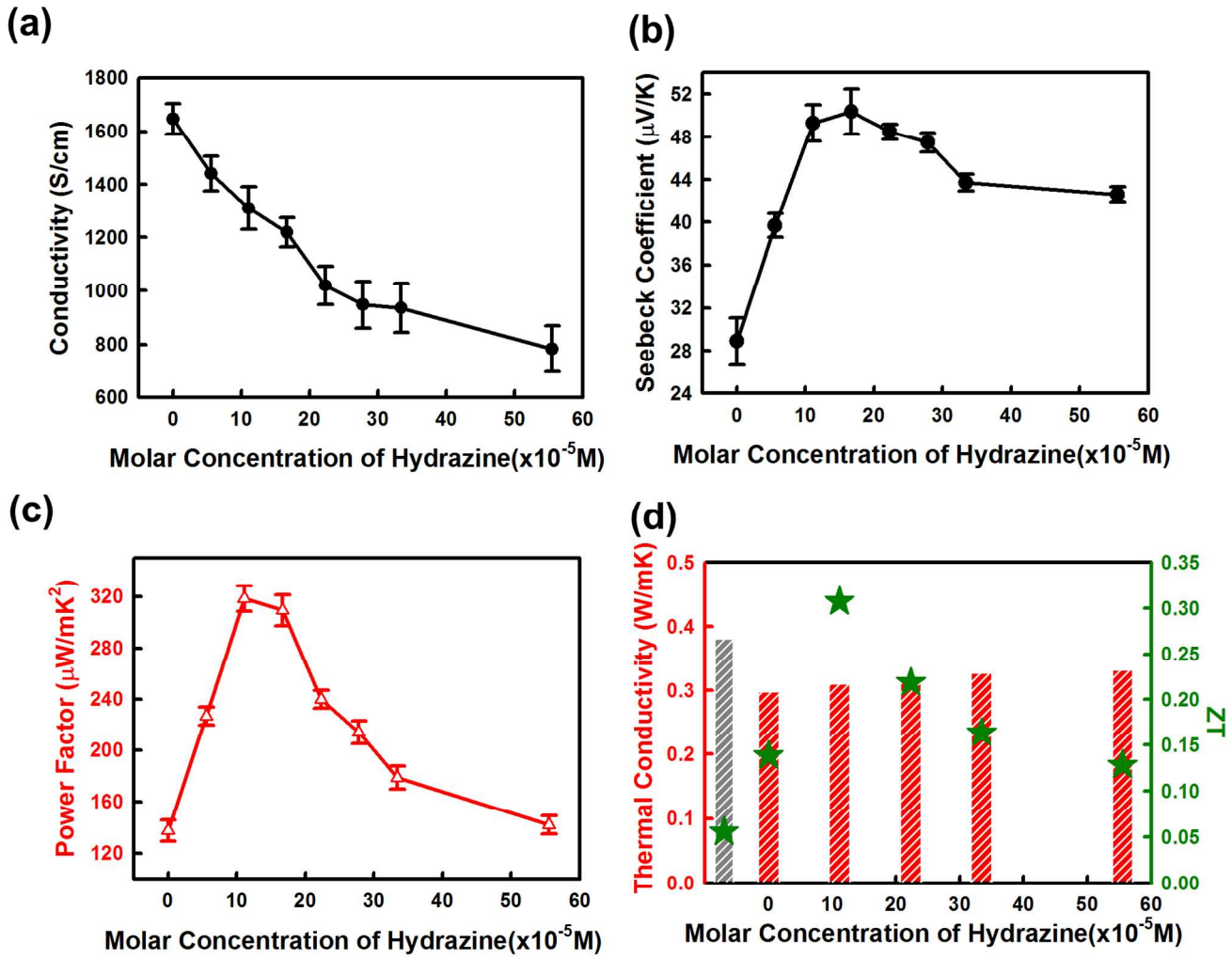

Fig 1. Thermoelectric properties of hydrazine/DMSO-dedoped PEDOT:PSS (DDTP) films as a function of hydrazine concentration: (a) electrical conductivity (σ); **(b)** Seebeck coefficient (S); (c) power factor ($S^2 \bullet \sigma$); (d) thermal conductivity (κ) and ZT.

The investigation of the hydrazine/DMSO dedoping on the thermoelectric properties of DTP-100 PEDOT:PSS films is shown in Fig 1. Fig. 1(a) shows the variation of σ values of the films treated with hydrazine/DMSO solution (DDTP) as a function of hydrazine concentration, from 0 to 5.55×10^{-4} M. When DTP-100 is treated with pure DMSO (DDTP-0), σ increased to 1647 S/cm, ~400 S/cm higher than the pristine DTP-100 film (σ = 1218 S/cm). In contrast, σ of DDTP films continuously decreases from 1647 S/cm to 783 S/cm as the hydrazine concentration increases from 0 to 5.55×10^{-4} M. As shown in mention above, the electrical conductivity (σ) is proportional to $n\times\mu_H$. The plots of n and μ_H as a function of hydrazine concentration are shown in Fig S1 (see the SI file). The σ increase of DDTP-0 is attributed to the washing of PSS by DMSO – PSS is an insulator hence its removal increases μ_H. This effect also occurs in the presence of hydrazine but it is offset by the much larger (by orders of magnitude) decrease of n caused by hydrazine. Overall, dedoping with a high hydrazine concentration leads to neutral PEDOT with a low concentration of PSS, which is characterized by low σ.

Fig. 1(b) shows the Seebeck coefficient of DDTP films as a function of hydrazine concentration. The Seebeck coefficient steeply increases and reaches a maximum value of 50.4 μV/K at hydrazine concentration of 1.67×10^{-4} M. Above this concentration, the Seebeck coefficient gradually decreases. Most significantly, the increase of the Seebeck coefficient is usually accompanied by the decrease in electrical conductivity.[34] During the hydrazine/DMSO dedoping, protonated hydrazine ions ($N_2H_5^+$) associate with PSS anions to minimize the Coulombic attraction between PEDOT and PSS, while DMSO washes PSS in the PEDOT:PSS film, and consequently the p-doping level of PEDOT decreases (Fig S2(a) in the SI file). For the materials with polaron-driven conductivity, the Seebeck coefficient is related to the charge carrier density (n) and the coefficient linearly decreases with a logarithmic increase of charge concentration.[34] Therefore, the Seebeck coefficient linearly increases as the hydrazine concentration increases from 0 to 1.67×10^{-4} M because n almost exponentially decreases (Fig S1 in the SI file). Above hydrazine concentration of 2.23×10^{-4} M, however, the Seebeck coefficient slightly decreases. An excess amount of hydrazine most likely denatures the PEDOT during the dedoping. Hydrazine molecules may attack the ethylenedioxy part of the EDOT unit via a tentative reduction mechanism (Fig S2(b) in the SI file), which hinders the electron transport hence decreases the thermoelectric power.[35] This 'over-reduction' was confirmed by a decrease in the PEDOT O 1s peak intensity in the XPS analyses of the DTP films treated with high concentrations of hydrazine. (Fig S3 in the SI file).

Fig. 1(c) shows the power factor ($S^2 \bullet \sigma$) of the DDTP films as a function of hydrazine concentration. The power factor of the DTP film treated with pure DMSO (DDTP-0) is 137.6 μW/mK^2, which is higher than that of pristine DTP films (70.7 μW/mK^2, DTP-100). When the hydrazine concentration increases from 0 to 1.11×10^{-4} M, the power factor increases from 137.6 to 318.4 μW/mK^2, but it decreases again from 309.4 to 142.1 μW/mK^2 as the hydrazine concentration increases to 5.55×10^{-4} M. The above behavior can be rationalized by the synergistic effect of the optimal oxidation level and the electron mobility increase due to the decreased p-doping level of PEDOT and the removal of insulating PSS molecules.

Fig. 1(d) shows the thermal conductivity (κ) and the thermoelectric figure of merit (ZT) for DDTP films as a function of hydrazine concentration. The κ value decreases from 0.38 to 0.30 Wm^{-1}K^{-1} under the optimal dedoping conditions by removal of insulating PSS. Thermal conductivity of conducting polymers are dominated by the phonon transport hence it can be affected by dopants that may alter the heat capacity and the density of the polymer.[29] The removal of PSS from PEDOT:PSS film decreases the specific heat (C_p) (Table S1), resulting in thermal conductivity decrease.[27] Under the same conditions (1.11×10^{-4} M hydrazine concentration), the ZT value and the power factor reached 0.31 and 318.4 μW/mK^2, respectively, at room temperature.

The PSS in PEDOT:PSS plays important roles as a stabilizer in PEDOT preparation, a primary dopant in *p*-doping of PEDOT and a binder in PEDOT coating. However, PSS lowers the Seebeck coefficient by increasing the carrier concentration; therefore, excess PSS should be removed. Hydrazine/DMSO treatment during the spin coating was found to be quite effective in terms of selective PSS removal with a simultaneous control of the PEDOT oxidation level.

Fig. 2(a) shows the thickness of the TSA-doped PEDOT:PSS film and the films treated with hydrazine/DMSO as a function of hydrazine concentration. The film thickness decreases after spin coating with hydrazine/DMSO as the hydrazine concentration increases due to the removal of PSS molecules as confirmed by XPS analysis. As shown in Fig. 2(b), the S 2p peaks in the XPS spectra separate into two bands. The lower (164.6 and 163.4 eV) and the higher (169 and 167.8 eV) energy peaks correspond to the S atoms in PEDOT and PSS, respectively.[36, 37] The intensity of the S 2p PEDOT peak in XPS spectra normalized to the sulfur peak at 168.8 eV increases as the hydrazine concentration increases, implying that the relative amount of PEDOT relative to PSS increases.

The PSS in PEDOT:PSS plays important roles as a stabilizer in PEDOT preparation, a primary dopant in *p*-doping of PEDOT and

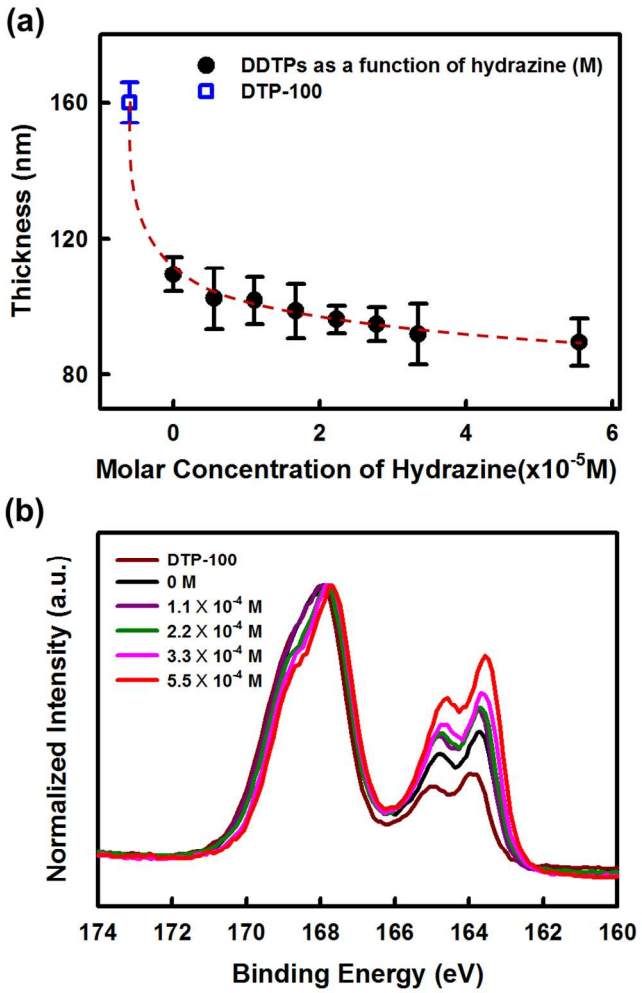

Fig 2. (a) Thickness of the doped PEDOT:PSS film (DTP-100) and hydrazine/DMSO-dedoped PEDOT:PSS films (DDTPs) as a function of hydrazine concentration. (b) S 2p XPS spectra of the DDTP films normalized to the 168.8 eV (S 2p from PSS) peak.

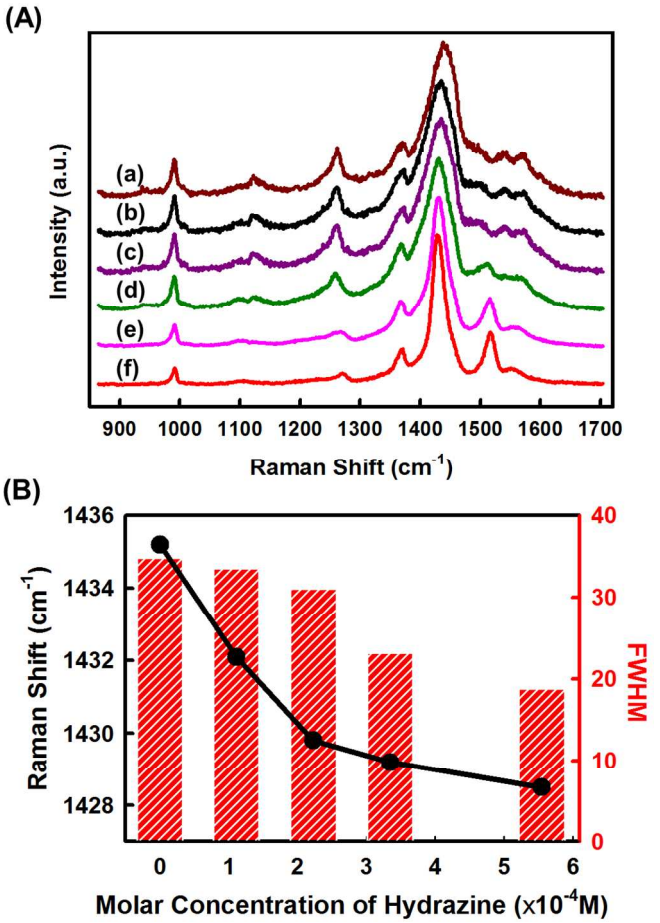

Fig 3. (A) Raman spectra of hydrazine/DMSO-dedoped PEDOT:PSS films (DDTPs) as a function of hydrazine concentration: (a) DTP-100; (b) 0 M; (c) 1.11×10^{-4} M; (d) 2.22×10^{-4} M; (e) 3.33×10^{-4} M; and (f) 5.55×10^{-4} M. The excitation wavelength was 514 nm. (B) Blue shift and full width at half maximum (FWHM) of the peak at 1436 – 1428 cm^{-1} as a function of hydrazine concentration.

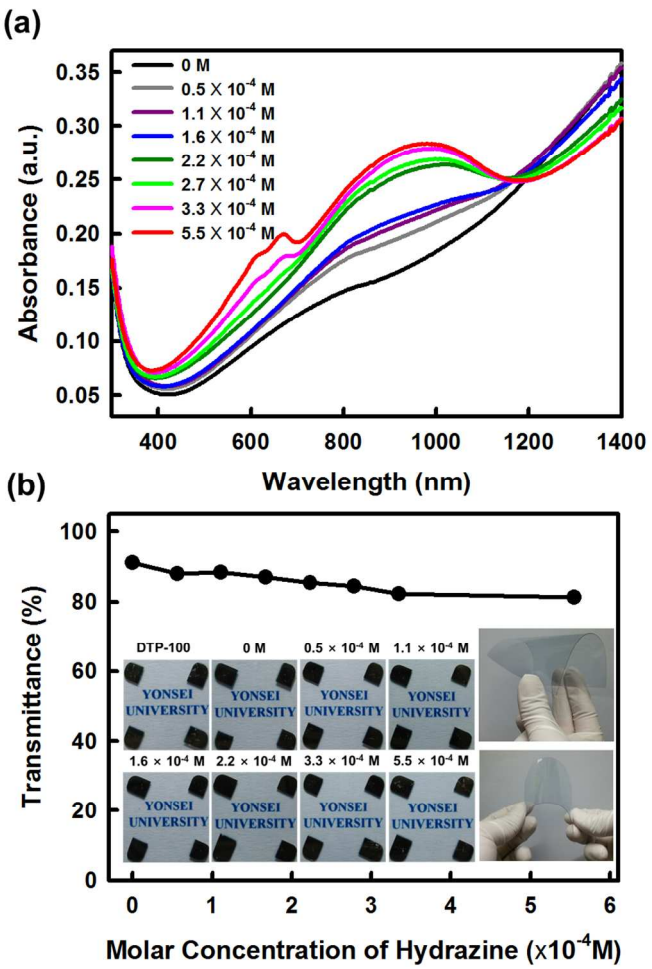

Fig 4. (a) The UV-Vis-NIR absorption spectra of hydrazine/DMSO-dedoped PEDOT:PSS films (DDTPs). (b) Transmittance at 550 nm as a function of hydrazine concentration. The insets show photographic images of 4 gold electrode-patterned DDTP films with different transmittance and the flexible DDTP-coated PET films.

a binder in PEDOT coating. However, PSS lowers the Seebeck coefficient by increasing the carrier concentration; therefore, excess PSS should be removed. Hydrazine/DMSO treatment during the spin coating was found to be quite effective in terms of selective PSS removal with a simultaneous control of the PEDOT oxidation level.

The Raman spectra (514 nm Ar laser) of PEDOT:PSS films treated with hydrazine/DMSO during spin coating (DDTP films) are shown in Fig. 3. In general, peak shifting to higher wavenumbers is due to doping level increase. This effect is related to the degree of backbone deformation during oxidation to polarons and bi-polarons and the associated transitions between quinoid- and benzoid-dominated forms.[38] The strong band assigned to the symmetric C_α=C_β stretch at 1436 cm^{-1} shifts to 1428 cm^{-1} with simultaneous peak narrowing as the hydrazine concentration increases (Fig. 3 inset). This Raman shift implies that PEDOT oxidation level decreases from bipolaron to polaron or neutral by hydrazine/DMSO dedoping. Also, a moderately intense band near 1516 cm^{-1} corresponding to the asymmetric C_α=C_β in-plane stretch[39] appears at hydrazine concentration of 3.34×10^{-4} M, while the peak at 1546 cm^{-1} disappears. These results suggest that hydrazine dedoping converts PEDOT chains into a chemically neutral state. Particularly, the intensities of the peaks at 991 and 1121 cm^{-1} decrease as hydrazine concentration increases, which indicates a decrease in the PSSconcentration.[40]

Fig. 4(a) shows the ultraviolet-visible-near-infrared (UV-Vis-NIR) absorption spectra of the PEDOT:PSS films. The optical spectra change systematically as a function of hydrazine concentration hence of the oxidation level. The NIR transitions above 900 nm are attributed to interacting bipolarons and those in the visible region (~600 nm) to π-π^* transition of neutral or dedoped PEDOT.[28, 41] As a result from the dedoping, bi-polaronic optical transitions (~1400 nm) gradually disappear, while the neutral (~600 nm) and polaron (~900 nm) transitions appear, consistent with the transition of PEDOT chains from bipolaron ($PEDOT^{2+}$) to polaron ($PEDOT^{+}$) and neutral ($PEDOT^{0}$) state.[28] Figure 4(b) shows the transmittance (in %) of the dedoped PEDOT:PSS coated on PET film as a function of hydrazine concentration. The transmittance value decreases slightly from 91 to 81 % as the hydrazine concentration increases to 5.55×10^{-4} M, with a simultaneous color change from light blue (higher oxidation level) to dark blue (lower level) due to oxidation level-dependent electrochromism.[42] The transmittance at the highest thermoelectric performance (at 1.11×10^{-4} M hydrazine concentration) is 88.3 %. The transparent PEDOT:PSS can be fabricated on wide areas of flexible PET film, which can be bent or twisted (Fig. 4b inset). Therefore, this film is suitable for thermoelectric devices.

Conclusions

In summary, a transparent and flexible thermoelectric nanofilms have been successfully fabricated from a PEDOT:PSS thin film; the PSS concentration and oxidation level of PEDOT are optimized by doping with DMSO/TSA and dedoping with hydrazine/DMSO. The former increases the electrical conductivity of PEDOT and the latter selectively removes the insulating barrier of PSS and controls the oxidation level of PEDOT. Under optimized concentrations of both dopants, the highest power factor of 318.4 $\mu W/mK^2$, the lowest κ of 0.30 W/mK, ZT of 0.31 and optical transmittance of 88.3 % at room temperature have been attained. The conducting polymer thin film has potential for applications in thermoelectric power devices where high-efficiency, transparency, flexibility, and large-area are required.

Acknowlegements

Support by the following institutions is gratefully acknowledged: Nano·Material Technology Development Program, National Research Foundation of Korea (NRF) funded by the Ministry of Education, Science and Technology (grant 2008-2002380/2012-0006227); Pioneer Research Center Program, National Research Foundation of Korea funded by the Ministry of Science, ICT & Future Planning (grant 2010-0019550) and the Ministry of Education, Science and Technology (grant 2009-0093823); National Research Foundation of Korea (NRF) funded by the government of Republic of Korea (MSIP) (grant 2007-0056091); Converging Center Program funded by the Ministry of Education, Science and Technology (grant 2010K001430).

Supporting Information

Characterization, table of thermal conductivity parameters, carrier concentration and charge mobility, detailed description of dedoping/reduction mechanism and XPS measurements.

Notes and references

[a]*Department of Chemical and Biomolecular Engineering, Yonsei University, 262 Seongsanno, Seodaemun-gu, Seoul 120–749, South*

Korea. Email:jayhkim@yonsei.ac.kr, Tel: +82-2-2123-7633, Fax: +82-2-312-0305
[b]*Department of Applied Chemistry, Kyungpook National University, 80 Daehak-ro, Buk-gu, Daegu 702–701, South Korea. Email: inwoo@knu.ac.kr*

1. K. Wang, H. Wu, Y. Meng, Y. Zhang, Z. Wei, Energy Environ. Sci. 2012, **5**, 8384-8389.
2. Dincer, I. Renew. Sust. Energ. Rev. 2000, **4**, 157-175.
3. M. Freitag, E. Galoppini, Energy Environ. Sci. 2011, **4**, 2482-2494.
4. K. Ahnert, M. Abel, M. Kollosche, P. J. Jørgensen, G. J. Kofod, Mater. Chem. 2011, **21**, 14492-14497.
5. K. Gupta, P. Tiwari, N. Gupta, Adv. Mater. Res. 2013, **685**, 161-165.
6. D. Liang, H. Yang, S. W. Finefrock, Y. Wu, Nano Lett. 2012, **12**, 2140-2145.
7. G. P. Moriarty, K. Briggs, B. Stevens, C. Yu, J. C. Grunlan, Energy Technology. 2013, **1**, 265-272.
8. G. Roy, E. Matagne, P. J. Jacques, Electron. Mater. 2013, **12**, 1-8.
9. G. J. Snyder, Thermoelectric energy harvesting (Energy Harvesting Technologies). 2009, **3**, 325-336.
10. Y. Sun, H. Cheng, S. Gao, Q. Liu, Z. Sun, C. Xiao, C. Wu, S. Wei, Y. J. Xie, Am. Chem. Soc. 2012, **134**, 20294-20297.
11. H. Yang, L. A. Jauregui, G. Zhang, Y. P. Chen, Y. Wu, Nano lett. 2012, **12**, 540-545.
12. Y. Yang, W. Guo, K. C. Pradel, G. Zhu, Y. Zhou, Y. Zhang, Y. Hu, L. Lin, Z. L. Wang, Nano lett. 2012, **12**, 2833-2838.
13. G. J. Snyder, E. S. Toberer, Nat. mater. 2008, **7**, 105-114.
14. G. Chen, K. Xu, D. J. Qiu, Mater. Chem. A. 2013. **1**, 12395- 12399.
15. N. E. Coates, S. K. Yee, B. McCulloch, K. C. See, A. Majumdar, R. A. Segalman, J. J. Urban, Adv. Mater. 2013, **25**, 1629-1633.
16. Y. Du, S. Z. Shen, K. Cai, P. S. Casey, Prog. Polym. Sci. 2012, **37**, 820-841.
17. N. Dubey, M. J. Leclerc, Polym. Sci., Part B: Polym. Phys. 2011, **49**, 467-475.
18. J. Li, X. Tang, H. Li, Y. Yan, Q. Zhang, Synth. Met. 2010, **160**, 1153-1158.
19. T. Stöcker, A. Köhler, R. J. Moos, Polym. Sci., Part B: Polym. Phys. 2012, **50**, 976-983.
20. D. K. Taggart, Y. Yang, S. C. Kung, T. M. McIntire, R. M. Penner, Nano lett. 2010, **11**, 125-131.
21. Q. Yao, L. Chen, W. Zhang, S. Liufu, X. Chen, ACS Nano 2010, **4**, 2445-2451.
22. B. Zhang, J. Sun, H. Katz, F. Fang, R. Opila, ACS Appl. Mater. Interfaces. 2010, **2**, 3170-3178.
23. R. Yue, J. Xu, Synth. Met. 2012, **162**, 912-917.
24. Y. Xuan, X. Liu, S. Desbief, P. Leclère, M. Fahlman, R. Lazzaroni, M. Berggren, J. Cornil, D. Emin, X. Crispin, Phys. Rev. B: Condens. Matter. 2010, **82**, 115454.
25. R. Yue, S. Chen, C. Liu, B. Lu, J. Xu, J. Wang, G. J. Liu, Solid State Electrochem. 2012, **16**, 117-126.
26. D. Antiohos, G. Folkes, P. Sherrell, S. Ashraf, G. G. Wallace, P. Aitchison, A. T. Harris, J. Chen, A. I. Minett, J. Mater. Chem. 2011, **21**, 15987-15994.
27. G. H. Kim, L. Shao, K. Zhang, K. P. Pipe, Nat. mater. 2013, **12**, 719-723.
28. O. Bubnova, Z. U. Khan, A. Malti, S. Braun, M. Fahlman, M. Berggren, X. Crispin, Nat. mater. 2011, **10**, 429-433.
29. O. Bubnova, X. Crispin, Energy Environ. Sci. 2012, **5**, 9345
30. J. Luo, D. Billep, T. Waechtler, T. Otto, M. Toader, O. Gordan, E. Sheremet, J. Martin, M. Hietschold, D. R. T. Zahn, T. J. Gessner, Mater. Chem. 2013, **1**, 7576–7583.
31. M. He, F. Qiu, Z. Lin, Energy Environ. Sci. 2013, **6**, 1352-1361.
32. S. H. Yu, J. H. Lee, M. S. Choi, J. H. Park, P. J. Yoo, J. Y. Lee, Mol. Cryst. Lig. Cryst. 2013, **580**, 76-82.
33. H. Mao, X. Wu, X. Qian, X. An, Cellulose. 2014, 21, 697-704.
34. T. C. Tsai, H. C. Chang, C. H. Chen, W. T. Whang, Org. Electron. 2011, **12**, 2159-2164.
35. R. R. Heikes, R. W. Ure, Thermoelectricity (Interscience, New York). 1961. **4**, 77.
36. H. Kim, S. Nam, H. Lee, S. Woo, C. S. Ha, M. Ree, Y. Kim, J. Phys. Chem. C. 2011, **115**, 13502-13510.
37. Y. H. Kim, C. Sachse, M. L. Machala, C. May, L. Müller-Meskamp, K. Leo, Adv. Funct. Mater. 2011, **21**, 1076-1081.
38. M. De Kok, M. Buechel, S. Vulto, P. Van de Weijer, E. Meulenkamp, S. De Winter, A. Mank, H. Vorstenbosch, C. Weijtens, V. Van Elsbergen, Phys. Status Solidi A. 2004, **201**, 1342-1359.
39. S. Garreau, G. Louarn, J. Buisson, G. Froyer, S. Lefrant, Macromolecules 1999, **32**, 6807-6812.
40. M. Stavytska-Barba, A. M. Kelley, J. Phys. Chem. C. 2010, **114**, 6822-6830.
41. J. C. Gustafsson, B. Liedberg, O. Inganäs, Solid State Ionics 1994, **69**, 145-152.
42. D. Mecerreyes, R. Marcilla, E. Ochoteco, H. Grande, J. A. Pomposo, R. Vergaz, J. M. Sánchez Pena, Electrochim. Acta. 2004, **49**, 3555-3559.

